Hydrogenated Amorphous-Silicon/Crystalline-Silicon Heterojunctions: Properties and Applications

HIDEHARU MATSUURA

Abstract—**Fundamental properties of amorphous silicon/crystalline-silicon heterojunctions are studied through their capacitance–voltage (C–V) and current–voltage (I–V) characteristics. In light of the heterojunction properties, applicability to devices such as vidicon targets, gamma-ray detectors, solar cells, and heterojunction bipolar transistors is discussed.**

I. Introduction

HYDROGENATED amorphous silicon (a-Si:H) has been a highly important material for device applications. In order to make use of both the good properties of a-Si:H and crystalline silicon (c-Si), electric and photoelectric properties of a-Si:H/c-Si heterojunctions have been intensively studied. Various models [1]–[3] were proposed to explain capacitance–voltage (C–V) or current–voltage (I–V) characteristics of a-Si:H/c-Si heterojunctions. In this paper, typical C–V and I–V characteristics are discussed in a simple structure of an undoped a-Si:H/p-type c-Si (p c-Si) heterojunction, and the action mechanisms as well as the advantages of a variety of devices utilizing these heterojunctions are then explained on the basis of their fundamental properties.

II. Fundamental Properties of a-Si:H/c-Si Heterojunctions

A. Sample Preparation

In order to fabricate a simple heterojunction diode, gold (Au) was evaporated onto a back side of p c-Si with the acceptor density of 10^{16} cm^{-3}, and p c-Si with evaporated Au was then heated up to 400°C for 1 min in order to get a good ohmic contact between the p c-Si and the Au. An undoped a-Si:H film (about 1.2 μm thick) was deposited by glow-discharge (GD) decomposition of pure SiH_4 gas onto the p c-Si surface that was heated to 260°C. Magnesium (Mg) was evaporated on the a-Si:H film with an area of 0.785 mm^2 at room temperature since Mg is known to form a good ohmic contact with undoped a-Si:H [4]. A structure of the heterojunction is schematically shown in the inset of Fig. 1.

B. Capacitance–Voltage Characteristics

Fig. 1 shows the high-frequency (1 MHz) C–V characteristics of the heterojunction, showing typical high-frequency C–V characteristics of amorphous/crystalline heterojunctions. Two analyses were proposed in order to explain these C–V characteristics: 1) a metal-oxide-semiconductor (MOS)-type analysis [1], where a-Si:H behaves like an oxide layer; and 2) a p-n junction-type analysis [2], [5]. The essential difference between them is as follows. In the MOS-type analysis, the quasi-Fermi level for electrons is assumed to coincide with the quasi-Fermi level for holes in the depletion region, which means that the Fermi level can be defined even in the depletion region at any applied voltage. Therefore, this analysis should be applied to a heterojunction across which a current does not flow. In the p-n junction-type analysis, on the other hand, the quasi-Fermi level for electrons is separated from the quasi-Fermi level for holes in the depletion region when a voltage is applied across the junction. Therefore, the p-n junction-type analysis should be applied to a heterojunction across which a current does flow. Since this heterojunction behaves like a p-n heterojunction (which is mentioned in Sections II-E and F), these C–V characteristics should be discussed by the p-n junction-type analysis.

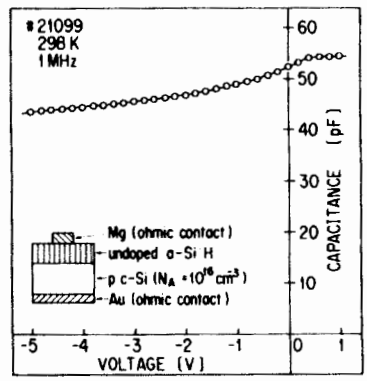

Fig. 1. Capacitance–voltage characteristics of the undoped a-Si:H/p c-Si heterojunction.

The depletion region formed by the heterojunction is taken into consideration. When a reverse bias voltage is applied, it produces space-charge layers both in a-Si:H and in c-Si. Since this p c-Si has only shallow acceptors, the space charge in the p c-Si is formed by negatively charged acceptors. However, localized states in a-Si:H distribute within the gap. Let us discuss the origin of the positive space charge in a-Si:H using Fig. 2. In the neutral region, all the gap states below the Fermi level (E_F)

Manuscript received November 22, 1988; revised July 30, 1989.
The author is with the Electrotechnical Laboratory, Ibaraki, Japan.
IEEE Log Number 8931496.

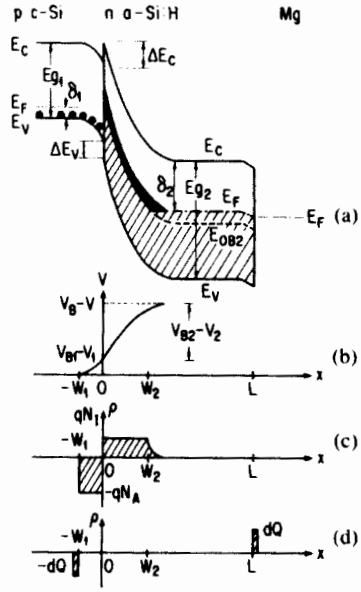

Fig. 2. Schematic sketches of the heterojunction; (a) energy-band diagram; (b) potential variation; (c) space-charge density for a reverse bias voltage; (d) charge in response to a small 1-MHz ac voltage to measure capacitance. The gap states as indicated by the black area behave like positively charged states, and the states as indicated by the hatched area of (a) are occupied by electrons.

are occupied by electrons, whereas in the depletion region, the gap states above E_{OB2} are devoid of electrons, where E_{OB2} is determined from the condition that the thermal emission rate for electrons is equal to that for holes and given by [5]

$$E_{OB2} = E_V + E_{g2}/2 + (kT/2)\ln(\nu_p/\nu_n) \quad (1)$$

where ν_p and ν_n are the attempt-to-escape frequencies for holes and electrons, respectively. Therefore, the gap states in the area painted in black in Fig. 2(a) behave like positive space charges (herein referred to as donor-like states). The density of the donor-like states is constant in the spatial position between 0 and W_2. This, together with the density of donors (if they exist), gives the effective density of the donor-like states (N_I), as shown in Fig. 2(c). Fig. 2(b) shows the potential variation with distance where V_B is the built-in voltage. The depletion widths (W_1 and W_2) are given by

$$qN_AW_1 \cong qN_IW_2 \quad (2)$$

with

$$W_1 = \left[2\epsilon_{s1}(V_{B1} - V_1)/qN_A\right]^{1/2} \quad (3)$$

and

$$W_2 \cong \left[2\epsilon_{s2}(V_{B2} - V_2)/qN_I\right]^{1/2}. \quad (4)$$

Here, ϵ_s is the semiconductor permittivity. In Fig. 2(a), δ is the energy difference between the Fermi level and the nearest band edge, E_g the energy bandgap, W the width of the depletion region, L the thickness of a-Si:H, and ΔE the discontinuity in energy between band edges of the two semiconductors. The subscripts 1 and 2 refer to p c-Si and a-Si:H, respectively, and the subscripts C and V refer to the conduction band and the valence bond, respectively.

The capacitance was measured with a small ac voltage at 1 MHz. The resistivity ρ_1 of this p c-Si is about 1 Ωcm so that the dielectric relaxation time ($\epsilon_{s1}\rho_1$) becomes 10^{-12} s, indicating that the capacitance C_1 in c-Si is given by

$$C_1 = \epsilon_{s1}/W_1. \quad (5)$$

On the other hand, the resistivity ρ_2 of undoped a-Si:H used is about 10^9 Ωcm. Then, the dielectric relaxation time becomes 10^{-3} s, suggesting that the undoped a-Si:H film acts as a dielectric material under the 1-MHz ac voltage; therefore, the capacitance C_2 in a Si:H can simply be given by:

$$C_2 = \epsilon_{s2}/L. \quad (6)$$

The measured capacitance C at 1 MHz is expressed as:

$$1/C = 1/C_1 + 1/C_2 \quad (7)$$

because the redistribution of charge can spatially respond to the 1-MHz ac voltage at W_1 and L, as shown in Fig. 2(d). From (2)–(4), the following equation is obtained:

$$(V_{B1} - V_1)/(V_{B2} - V_2) \cong N_I\epsilon_{s2}/N_A\epsilon_{s1}. \quad (8)$$

Finally, the next equations are derived from (3), (5), (7) and (8):

$$W_1^2 = \left\{\epsilon_{s1}(1/C - 1/C_2)\right\}^2 \quad (9)$$

$$\cong 2\epsilon_{s1}\epsilon_{s2}N_I(V_B - V)/qN_A(N_A\epsilon_{s1} + N_I\epsilon_{s2}). \quad (10)$$

Fig. 3 shows the W_1^2 versus V relationship, which was replotted from the data in Fig. 1. The data reveal a good linear relationship, indicating that the p-n junction-type analysis is applicable to the present system. As is clear from (10), values of N_I and V_B can be graphically determined from the slope of the line and the intercept on the abscissa, respectively. From Fig. 3, for example, N_I and V_B were 3×10^{15} cm^{-3} and 0.35 V, respectively. The number of the a-Si:H/c-Si interface states is important for discussing the validity of N_I, but the experimental determination of the number is quite difficult. However, although the straight line could not be obtained in the low reverse bias region ($0\ V < V < -2\ V$) if the interface states affected the C–V characteristics very much, the straight line was obtained as shown in Fig. 3. On simple calculation, N_I of 3×10^{15} cm^{-3} is close to the real bulk density when the number of the interface states is smaller than 10^{11} cm^{-2}. Since N_I value obtained from Fig. 3 was close to the bulk spin density obtained from electron-spin-resonance (ESR) measurements of the specimens prepared from the identical deposition conditions where surface state contributions were estimated by results from a series of films over a range of thicknesses, N_I is thought to represent the density of singly occupied dangling bonds.

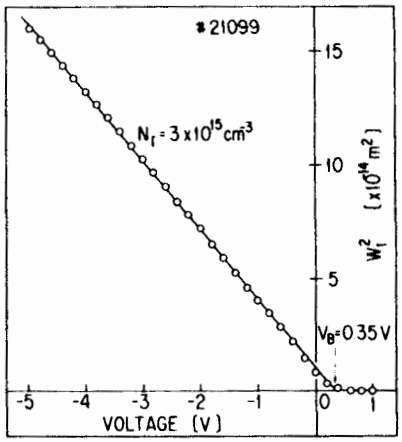

Fig. 3. Width of the depletion region in p c-Si as a function of bias voltage.

C. Band Discontinuity

The conduction-band discontinuity is expressed by

$$\Delta E_C = \delta_1 + \delta_2 - E_{g1} + qV_B \tag{11}$$

where δ_1 is estimated from N_A, and δ_2 is obtained as the activation energy of dark conductivity of a-Si:H. From Fig. 3, ΔE_C was estimated as 0.14 eV using $\delta_1 = 0.18$ eV, $\delta_2 = 0.73$ eV, and $E_{g1} = 1.12$ eV. The average value of ΔE_C in a lot of experimental data was 0.20 eV [2], indicating that the main-band discontinuity occurs in the valence band because $\Delta E_C + \Delta E_V = E_{g2} - E_{g1}$. Similar results were recently obtained from a study of internal photoemission [6].

In the cases of sputtered (SP) a-Si:H [7] and evaporated (EV) amorphous silicon (a-Si) [8], however, ΔE_V was reported to be close to zero. The values of ΔE_C and ΔE_V depend on properties of interface as well as structures of amorphous films (e.g., hydrogenated or not). Therefore, they are strongly correlated with the deposition methods, such as GD, SP, and EV.

D. Transient Capacitance

Fig. 4 shows the change in the capacitance of the heterojunction after a reverse bias voltage (-4 V) is applied to the sample under the zero-bias condition. Since a-Si:H possesses deep gap states whose emission rates are small, the capacitance gradually decreases with time t. From this transient behavior of capacitance, a density-of-state distribution $g(E)$ in undoped a-Si:H can be defined [5]. This method may be a powerful technique for determining $g(E)$ in undoped a-Si:H because it has been difficult to obtain $g(E)$ in such a highly resistive material by the conventional transient capacitance method using Schottky-barrier diodes.

From (9) and (10), N_I at t can be expressed as

$$N_I(t) = qN_A^2\epsilon_{s1}W_1(t)^2/\left[2\epsilon_{s1}\epsilon_{s2}(V_B - V) - qN_A\epsilon_{s2}W_1(t)^2\right] \tag{12}$$

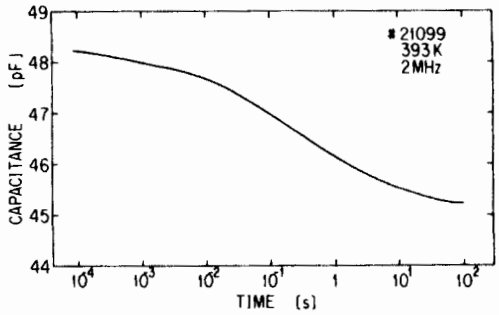

Fig. 4. Transient capacitance.

with

$$W_1(t) = \epsilon_{s1}(1/C(t) - 1/C_2) \tag{13}$$

where $C(t)$ is the capacitance at t, and $W_1(t)$ is the depletion width in the c-Si at t. The function $H(t)$ is defined as:

$$H(t) \equiv t\left[d\Delta N_I(t)/dt\right] \tag{14}$$

with

$$\Delta N_I(t) \equiv N_I(t) - N_I(\infty). \tag{15}$$

On the other hand, $H(t)$ is theoretically derived as [5]

$$H(t) = \int_{E_V}^{E_C} [f(E) - F_\infty(E)]g(E)t[e_n(E) + e_p(E)] \cdot \exp\left\{-[e_n(E) + e_p(E)]t\right\}dE \tag{16}$$

where

$$f(E) = 1/\left\{1 + \exp\left[(E - E_F)/kT\right]\right\} \tag{17}$$

$$F\infty(E) = e_p(E)/\left[e_n(E) + e_p(E)\right] \tag{18}$$

$$e_n(E) = \nu_n \exp\left[(E - E_C)/kT\right] \tag{19}$$

and

$$e_p(E) = \nu_p \exp\left[(E_V - E)/kT\right]. \tag{20}$$

Finally, we can obtain $g(E)$ from the fitting procedure. In Fig. 5, the best-fit $g(E)$ for the sample is shown.

E. Forward Current–Voltage Characteristics

Fig. 6 shows the I–V characteristics [a) log I–log V, and b) log I–V plots] of the heterojunction and also shows typical I–V characteristics of amorphous/crystalline heterojunctions. Two current transport mechanisms were proposed in order to explain these I–V characteristics: 1) a bulk-limited (space-charge-limited) current-transport mechanism [3] and 2) a junction-limited current-transport mechanism [2]. The essential difference between them is whether the resistance of the depletion region is greater or smaller than that of the amorphous film. Namely, a bias voltage is applied across the whole range of amorphous film in the bulk-limited case, and it is applied across the depletion region in the junction-limited case.

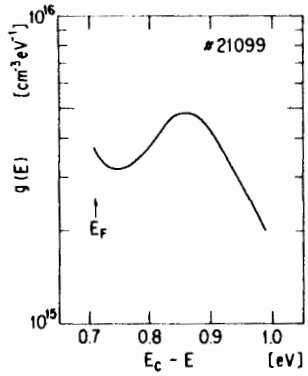

Fig. 5. Density-of-state distribution in undoped a-Si:H.

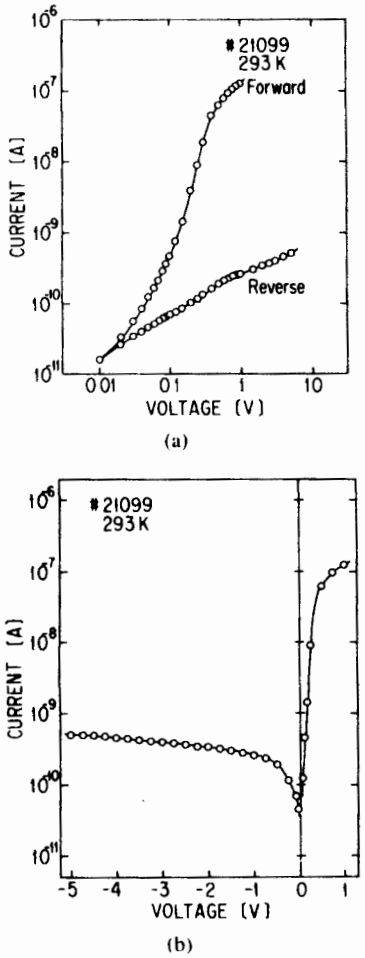

Fig. 6. Current-voltage characteristics; (a) log I-log V plots and (b) log I-V plots.

Since the resistivity and thickness of this a-Si:H were about 10^9 Ωcm and about 1.2 μm, respectively, the current expected from the resistance of the a-Si:H is about 3.3×10^{-9} A at 0.05 V for an area of 0.785 mm^2. Although the current at forward voltages lower than 0.05 V seems to be an ohmic current in Fig. 6(a) because $I \propto V$, the current at 0.05 V is much smaller than 3.3×10^{-9} A. Judging from the magnitude of the current, the forward current at <0.4 V is thought to be limited by the heterojunction. The voltage dependence of the junction-limited current can be expressed as:

$$I \propto \exp(AV) - 1 \tag{21}$$

where A is independent of the voltage. The current seems to be proportional to V lower than 0.05 V because $\exp(AV)$ can approximately expand $1 + AV$ in Taylor's series at $V < 0.05$ V.

Three models for explaining the current of heterojunctions are presented: 1) A is independent of the measuring temperature T for a tunneling model, 2) $A = q/kT$ for a diffusion model, and 3) $A = q/2kT$ for a recombination model. Fig. 7 shows the temperature dependence of the forward current from which the following relation could be obtained:

$$I = I_0 \exp(AV) \tag{22}$$

with

$$I_0 \propto \exp(-\Delta E_a/kT) \tag{23}$$

where ΔE_a is the activation energy of I_0. Because A is independent of T, the forward current is limited by a tunneling process.

The localized states are quasi-continuously distributed within the gap of a-Si:H spatially as well as energetically. It is reasonable to expect a multistep tunneling process to be dominant rather than a one-step tunneling process since the probability of multistep tunneling is much greater than that of one-step tunneling [9]. In order to explain these I-V characteristics, a multistep-tunneling capture-emission process [2] was proposed, as expressed in the inset of Fig. 7. A hole in the valence band of p c-Si flows from one localized state to another in a-Si:H by a multistep tunneling process, and it keeps flowing near the edge of the depletion region of a-Si:H. This hole is then recombined with an electron in the conduction band of a-Si:H, or it is emitted to the valence band of a-Si:H. This multistep tunneling process leads to the voltage dependence in (22), whereas the temperature dependence in (23) arises from either recombination or emission process of the tunneling hole. This model is now widely supported by other groups [10], [11].

F. Reverse Current-Voltage Characteristics

The a-Si:H/c-Si heterojunction can keep a dark current small even at a higher reverse bias voltage range, as is shown in Fig. 6. From (21) and (22), a saturated value of the reverse current is expected to be I_0. However, the reverse current exceeds the value of I_0, indicating that the reverse current should be limited by another transport mechanism. Fig. 8 shows the reverse current as a function of $(V_B - V)^{1/2}$, which is replotted from the data of Fig. 6. When the generation current is taken into account in the depletion region, this current should be proportional to the width of the depletion region that varies with $(V_B - V)^{1/2}$. The data show a good linearity in the range of

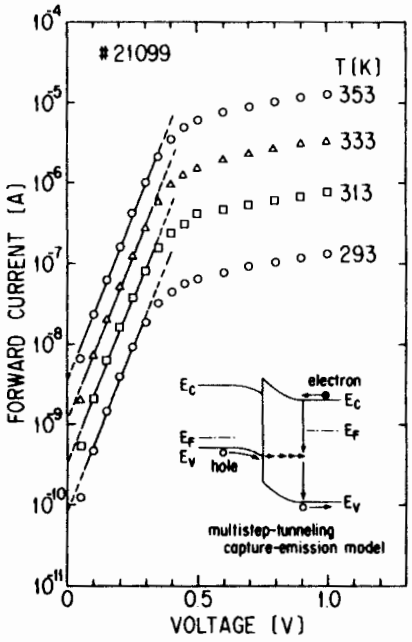

Fig. 7. Temperature dependence of the forward current. The schematic diagram for a multistep-tunneling capture-emission model is inserted.

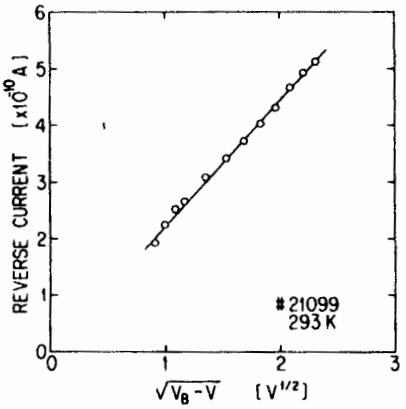

Fig. 8. Reverse current as a function of $(V_B - V)^{1/2}$, where V_B was 0.35 V.

$-0.5\ \text{V} < V < -5\ \text{V}$, indicating that this reverse current is limited by the generation current in the depletion region.

III. Applications of Heterojunctions

A. Vidicon Targets Without a p-n Diode Array

As an ultrahigh-photosensitive image-pickup tube, a silicon-intensifier target (SIT) tube with a p-n diode-arrayed c-Si target has been widely used. In this SIT tube, photoelectrons produced on the photoelectric surface are accelerated, and they generate a lot of electron-hole pairs in c-Si, which changes the charging condition on the scanning-electron-landing surface. This is the action mechanism of the conventional SIT tube. Disadvantages of the conventional SIT tube with a p-n diode-arrayed c-Si target are 1) the blooming effect due to the diffusion of excess carriers into adjacent p-n diodes, 2) the low resolution limited by the pitch of the diode array, and 3) the picture defects introduced in the fabrication process, which includes a high-temperature process for making p-n junctions. As a matter of course, the heterojunction targets such as c-Si/CdTe and c-Si/Sb_2S_3 without a diode array were proposed, but these heterojunctions did not exhibit rectifying properties that were good enough to get a high photo-to-dark current ratio.

The a-Si:H/c-Si heterojunction, in this sense, has the following advantages: 1) the heterojunction has a good rectifying property, indicating a small dark current under a large reverse bias condition; 2) the depletion region in c-Si, where the electron-hole separation takes place, spreads widely in the reverse bias condition, resulting in a large photocurrent. These are the advantages for getting a high signal-to-noise (S/N) ratio. In addition to the advantages in the action mechanism, the low-temperature process for the fabrication of the heterojunction is another advantage for preventing the defect formation in c-Si.

Fig. 9 shows a schematic diagram of a vidicon target having an a-Si:H/c-Si heterojunction [12]. Electrons thermally emitted from a cathode land on the surface of Sb_2S_3 (about 500 Å thick), and an electron-charged layer appears. The highly resistive boron (B)-doped a-Si:H layer ($B_2H_6/SiH_4 = 2.5 \times 10^{-5}$) prevents the electrons from flowing into the c-Si side. The charged condition of this surface is kept in the dark until next scanning electrons come to this spot (about 0.03 s). When the c-Si side is illuminated, electron-hole pairs are mainly generated in c-Si. The electric field formed by the n^+ c-Si/n c-Si contact enhances the separation of electron-hole pairs generated near this contact. The holes separated by the heterojunction move to the Sb_2S_3 layer. The a-Si:H layer also prevents those holes from diffusing in parallel to the surface because of a low diffusion coefficient of a-Si:H. The holes are recombined with the electrons, resulting in the change in the charging condition on the surface of Sb_2S_3. When scanning electrons come to this area again, a current flows in the circuit.

The actual reported values for this kind of vidicon are as follows [12]: the dark reverse current and sensitivity were 10 nA and 430 nA/lux at −6 V, respectively, which reach the values of well-defined c-Si targets with the p-n diode array; the horizontal resolution was attained to be more than 800 television lines, and the picture obtained had few defects, no blooming, and no burning, which makes it superior to those of the conventional c-Si vidicon target.

B. Gamma-Ray Detectors

A γ-ray detector requires a high-absorption coefficient for γ-ray, a wide depletion region, and a small dark reverse current. Although crystalline semiconductors (c-Ge, c-HgTe, and c-GaAs) consisting of atoms having heavy masses are suitable materials for γ-ray absorption, c-Si is considered to be the appropriate material for the γ-ray (< 100 keV) detector at the present stage because one expects to easily get a small dark reverse current as well

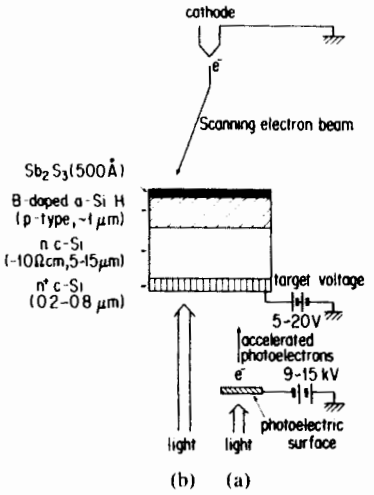

Fig. 9. Schematic sketches; (a) an SIT tube and (b) a vidicon target tube.

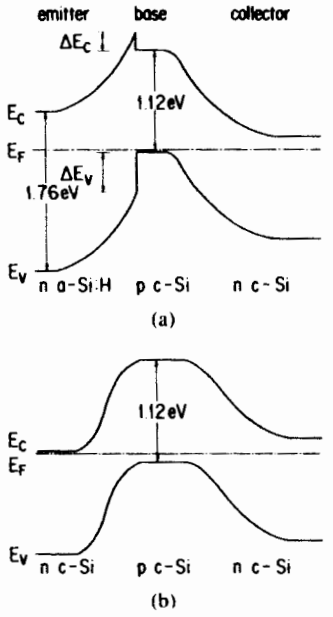

Fig. 10. Schematic sketches; (a) an n-p-n a-Si:H/c-Si/c-Si heterojunction bipolar transistor and (b) an n-p-n c-Si homojunction bipolar transistor.

as a wide depletion region due to its ultralow-impurity and defect levels. However, a high-temperature process such as solid-state diffusion of impurities or ion implantation followed by annealing to form a p-n homojunction (which produces additional defects in ultra-high purity c-Si, resulting in an increase of the dark reverse current and a decrease of the depletion region), is required.

The a-Si:H/c-Si heterojunction γ-ray detector has advantages such as low temperature and simple fabrication processes and good junction properties. An undoped a-Si:H/p c-Si heterojunction [13] was fabricated as follows. Undoped a-Si:H (1-μm thick) was deposited by GD decomposition of SiH_4 gas onto ultrahigh-purity p c-Si (300 μm thick with the resistivity higher than 10 kΩcm) heated to 200°C. Aluminum was evaporated on the a-Si:H film. The characteristics of this heterojunction γ-ray detector were reported to attain those comparable with c-Si detectors with a p-n homojunction. Moreover, this γ-ray detector can easily be applied to X-ray detectors.

C. Solar Cells

Similar to Schottky barrier (SB) and metal-thin insulator-semiconductor (MIS) solar cells, amorphous/crystalline-heterojunction solar cells have advantages such as simple and low-temperature fabrication processes, resulting in low-cost fabrication. In order to improve a low open circuit voltage in SB solar cells, a very thin oxide layer (about 20 Å) is needed between the metal and the semiconductor. However, it is quite difficult to control the thickness of such a thin oxide layer. It is expected, from this point of view, that the amorphous/crystalline-heterojunction solar cell shows reproducible and stable properties because the cell does not require any oxide layer. Actually, heterojunction solar cells were reported [14]. In B-doped a-SiC:H/n c-Si solar cells [15], the open-circuit voltage of 0.54 V, the short-circuit current of 30 mA/cm^2, and the efficiency of 11.38 percent under AM1 light (100 mW/cm^2) were achieved.

D. Heterojunction Bipolar Transistors

Advantages of HBT with a wide-bandgap emitter arise from the discontinuities (ΔE_V and ΔE_C) between the two semiconductors. Fig. 10 shows the energy-band diagram of an n a-Si:H/p c-Si/n c-Si transistor compared with that of a c-Si homojunction transistor. Since the large barrier in the valence band between a-Si:H and c-Si effectively prevents any holes from reaching the a-Si:H, the base doping level can be higher, and the emitter doping level can be lower. A high common-emitter-current gain h_{FE} defined by $\partial I_C/\partial I_B$ (I_C is the collector current, and I_B is the base current) is obtained because an injection efficiency is still closer to unity.

In general, the frequency response of transistors is limited by the carrier-transit time through the base layer. The HBT, in this sense, shows an advantage for a high-speed operation because the base layer can be designed to be thinner due to its higher doping level. High-speed HBT with a crystalline/crystalline heterojunction was tried in the field of Si-LSI. However, c-GaP as an emitter acts as a source of undesirable dopants for c-Si, and c-SiC shows a large lattice mismatch with c-Si. Since the dopant of the base layer is diffused during the high-temperature growth process of an emitter, a low-temperature process for fabricating an emitter on c-Si is strongly desired. Therefore, a-Si:H or a-SiC:H is thought to be a suitable material for a wide-bandgap emitter. Using the n a-Si:H/p c-Si/n c-Si as shown in Fig. 10(a), a maximum h_{FE} was reported to be 14 at a base Gummel number (GN) of 1.35×10^{12} s/cm^4 [16]. The GN is defined as Q_B/D_B where Q_B is the number of impurities per unit area in the base, and D_B is the minority-carrier diffusion coefficient in the base, and this is inversely proportional to the minority-carrier-current density in the base. In the case of an n a-SiC:H em-

itter instead of a-Si:H, a maximum h_{FE} of 120 at a GN of about 10^{12} s/cm^4 was also reported [17]. Although the large barrier in the valence band did not completely block the flow of holes from the base into the emitter, these HBT's exceeded Si homojunction transistors in h_{FE}.

The high resistance of the amorphous emitter, however, gives some disadvantages, resulting in the reduction of the collector current density and the reduction of high-frequency characteristics. In order to avoid these problems, hydrogenated amorphous-microcrystalline mixed-phase Si (μc-Si:H) or a-SiC:H with microcrystalline Si have been investigated as a wide-bandgap emitter [18], [19].

IV. Conclusion

The a-Si:H/c-Si heterojunction has junction properties suitable for a variety of device applications such as 1) a high forward-to-reverse current ratio, 2) a small dark current even at a large reverse bias condition, 3) wide depletion regions in both a-Si:H and c-Si, and 4) large valence-band and small conduction-band discontinuities between a-Si:H and c-Si. Vidicon targets and γ-ray (and X-ray) detectors make good uses of 2) and 3), solar cells make good use of 1) and 3), and n-p-n HBT's make good use of 1) and 4). Another big advantage of this heterojunction is a low-temperature fabrication process.

Acknowledgment

The author wishes to acknowledge his gratitude to Dr. A. Matsuda for his critical reading of the manuscript. He would also like to thank Dr. K. Tanaka and Dr. H. Okushi for their valuable comments. He wishes to thank Prof. S Furukawa of the Tokyo Institute of Technology (TIT), Prof. Y. Hatanaka of Shizuoka University, Dr. H. Mimura of the Nippon Steel Corporation, Dr. K. Sasaki of the TIT, and Dr. N. Sato of the Fuji Electric Corporate Research and Development, Ltd., for kindly giving important information on those devices.

References

[1] G. Sasaki, S. Fujita, and A. Sasaki, "Gap-states measurement of chemically vapor-deposited amorphous silicon: High-frequency capacitance-voltage method," *J. Appl. Phys.*, vol. 53, pp. 1013-1017, 1982.

[2] H. Matsuura, T. Okuno, H. Okushi, and K. Tanaka, "Electrical properties of n-amorphous/p-crystalline silicon heterojunctions," *J. Appl. Phys.*, vol. 55, pp. 1012-1019, 1984.

[3] V. Smid, J. J. Mares, L. Stourac, and J. Kristofik, "Amorphous-crystalline heterojunctions," in *Tetrahedrally-Bonded Amorphous Semiconductors*, D. Adler and H. Fritzsche, Eds. New York: Plenum, 1985, pp. 483-500.

[4] H. Matsuura, A. Matsuda, H. Okushi, T. Okuno, and K. Tanaka, "Metal-semiconductor junctions and amorphous-crystalline heterojunctions using B-doped hydrogenated amorphous silicon," *Appl. Phys. Lett.*, vol. 45, pp. 433-435, 1984.

[5] H. Matsuura, "A novel method for determining the gap-state profile and its application to amorphous $Si_{1-x}Ge_x$:H films," *J. Appl. Phys.*, vol. 64, pp. 1964-1973, 1988.

[6] H. Mimura and Y. Hatanaka, "Energy-band discontinuities in a heterojunction of amorphous hydrogenated Si and crystalline Si measured by internal photoemission," *Appl. Phys. Lett.*, vol. 50, pp. 326-328, 1987.

[7] M. Cuniot and Y. Marfaing, "Energy band diagram of the a-Si:H/c-Si interface as determined by internal photoemission," *Phil. Mag.*, vol. 57, pp. 291-300, 1988.

[8] F. Patella *et al.*, "Photoemission studies of amorphous silicon heterostructures," in *Proc. Conf. Optical Effects Amorphous Semiconductors* (Salt Lake City, Ut), 1984, pp. 402-409.

[9] A. R. Riben and D. L. Feucht, "Electrical transport in n Ge-p GaAs heterojunctions," *Int. J. Electron.*, vol. 20, pp. 583-599, 1966.

[10] H. Mimura and Y. Hatanaka, "Electrical properties of p-type hydrogenated amorphous silicon-n-type crystalline gallium arsenide heterojunctions," *Japan. J. Appl. Phys.*, vol. 24, pp. L355-L357, 1985.

[11] Z. Y. Xu *et al.*, "The effect of the gap DOS in a-Si on the properties on the a-Si/c-Si heterojunction," *J. Non-Cryst. Solids*, vol. 97, 98, pp. 983-986, 1987.

[12] H. Mimura and Y. Hatanaka, "The use of amorphous-crystalline silicon heterojunctions for the application to an imaging device," *J. Appl. Phys.*, vol. 61, pp. 2575-2580, 1987.

[13] M. Yabe, N. Sato, and Y. Seki, "A new silicon nuclear radiation detector using a-Si:H/c-Si heterojunction," in *Proc. 4th Sensor Symp.* (Tsukuba, Japan), 1984, pp. 105-109.

[14] K. Okuda, H. Okamoto, and Y. Hamakawa, "Amorphous Si/polycrystalline Si stacked solar cell having more than 12% conversion efficiency," *Japan. J. Appl. Phys.*, vol. 22, pp. L605-L607, 1983.

[15] M. M. Rahman and S. Furukawa, "Preparation and performance of a novel structure amorphous SiC/crystalline Si solar cell," in *Tech. Dig. Int. PVSEC-1* (Kobe, Japan), 1984, pp. 171-174.

[16] M. Ghannam, J. Nijs, R. Mertens, and R. Dekeersmaecker, "A silicon bipolar transistor with a hydrogenated amorphous emitter," in *IEDM Tech. Dig.*, 1984, pp. 746-748.

[17] K. Sasaki, S. Furukawa, and M. M. Rahman, "A novel structure amorphous SiC emitter HBT using low temperature process," in *IEDM Tech. Dig.*, 1985, pp. 294-297.

[18] J. Symons, K. Baert, J. Nijs, and R. Mertens, "Amorphous and microcrystalline silicon bipolar heterojunction transistors," *J. Non-Cryst. Solids*, vol. 97, 98, pp. 1315-1318, 1987.

[19] K. Sasaki, T. Fukazawa, and S. Furukawa, "Micro-crystalline hetero-emitter with high injection efficiency for Si HBT," in *IEDM Tech. Dig.*, 1987, pp. 186-189.

*

Hideharu Matsuura was born in Kyoto, Japan, on February 5, 1958. He received the B.S. and M.S. degrees in electronic engineering from Kyoto University, Kyoto, Japan, in 1980 and 1982, respectively.

In 1982, he joined the Electrotechnical Laboratory, Ibaraki, Japan. Since then, he has been concerned with research on junction properties in amorphous semiconductors.